Lasers in Surgery and Medicine 29:18–22 (2001)

Near-Infrared Photo-Excited Emission From Tissues Treated at Different Temperature Levels

Jing Tang, MD, PhD, Gang Zhang, MS, Fanan Zeng, MS, Ping Pei Ho, PhD, and R. R. Alfano, PhD*
Institute for Ultrafast Spectroscopy and Lasers and New York State Center for Advanced Technology for Ultrafast Photonic Materials and Applications, Departments of Electrical Engineering and Physics, The City College of the City University of New York, New York, New York 10031

Background and Objective: There is a lack of methods to evaluate the extent of thermal treatment of biological tissue. The intensity of the near-infrared (NIR) emission photo-excitation was investigated from tissue undergoing different levels of heat treatment.
Study Design/Materials and Methods: Chicken muscle was heated in an oven at different temperature levels ranging from 40°C until burn-off. The spectral emission intensity from these heat-treated tissues was measured with a CCD camera and the intensity was calculated.
Results: The emission intensity increased proportionally with respect to the extent of treatment temperature until burning. Linear relationships between treatment temperature and the emission intensity from tissue samples were found in three temperature ranges: from 40 to 160°C, from 165 to 220°C, and from 225 to 250°C.
Conclusion: The change in tissue damage after heat treatment could be detected by measuring the NIR emission intensity from the thermally damaged tissues. Lasers Surg. Med. 29:18–22, 2001. © 2001 Wiley-Liss, Inc.

Key words: near-infrared emission; tissue thermal damage

INTRODUCTION

In the treatment of diseases, many medical procedures depend on the thermal response. These procedures involve (1) laser therapies, such as laser tissue welding for tissue reconstruction [1–3]; laser angioplasty and recanalization for cardiovascular diseases [4]; laser interstitial hyperthermia for destroying cancers [5]; photocoagulation for homeostasis and photovaporization for tissue ablation [6–9]; (2) radiofrequency ablation for treatment of cardiac arrhythmias [10–12]; and (3) electrosurgery, such as eletrocoagulation for homeostasis and electrovaporization for tissue cutting in the pro-operative procedures. In these procedures, the degree of heat applied determines the ultimate bio-reaction. Destructive bio-reactions are possible from protein degradation, denaturation, vaporization, carbonization, and burn-off. A real-time demonstration of target tissue thermal damage and temperature monitoring to control the heat source in order to improve the outcome for patients is important. An accurate diagnostic method is also needed to evaluate burn patients. At present, there are few methods to detect the extent of the thermal reaction after thermal treatment. Most rely on histology for information. Many thermally induced morphological changes are subtle. Readily detectable morphological markers of thermal changes produced in vitro at tissue temperatures below 60°C have not been described for routinely prepared tissue for light microscopy. Some thermally produced tissue changes are similar and cannot be distinguished from artifacts produced by histological preparation for light microscopy. Transmission electron microscopy (TEM) reveals tissue damage produced by heating, but the small tissue samples required for TEM do not allow for the evaluation of the entire lesion [13].

There are several natural fluorophores in tissue, such as tryptophan, collagen, elastin, flavins, and porphyrin. Emission can be detected from the tissue upon excitation with the light. In our previous work [14–15], the emission intensity under 632 nm laser excitation from heat-damaged tissues (treated with a water bath) was found to increase proportionally with temperature rise. A linear relationship between treatment temperature and emission intensity from tissue samples from 55 to 97°C was observed. The relationship indicates that the extent of local "wet" heated tissue damage at a given temperature could be detected by measuring the NIR emission intensity from the thermally damaged tissue.

In the present study, the changes in the NIR emission intensity under 632 nm photo-laser excitation of the heat-treated tissues at different temperature levels were investigated. The results offer a new way to detect the changes associated with the application of the local heat to the tissue and the extent of in situ thermal damage after the heat treatment.

MATERIALS AND METHODS

A schematic diagram of the emission intensity imaging measurement setup is shown in Figure 1. The 632 nm laser beam from a He-Ne laser (Melles Griot, Carlsbad, CA) was passed through a narrow band filter (NB) and then expanded by a holographic light shaping diffuser (LSD, Physical Optics Corp., Torrance, CA). The central portion

*Correspondence to: R.R. Alfano, Institute for Ultrafast Spectroscopy and Lasers Department of Physics, The City College of the City University of New York, 138th Street and Convent Avenue, New York, NY 10031.
Accepted 1 December 2000

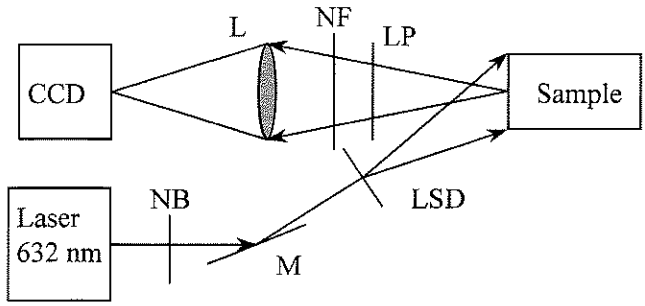

Fig. 1. Schematic diagram of NIR emission image measurement setup. NB: narrow band filter, M: mirror, LSD: holographic light shape diffuser, L: 50 mm camera lens, NF: laser line notch filter, LP: long pass filter.

of the expanded beam was used to illuminate the sample. The emitted light from the sample was collected by a 50 mm focal length camera lens (L_1) in the back-scattering geometry and imaged into a cooled charge-coupled device (CCD) camera (Photometrics CH350, Tucson, AZ). A CCD camera is a version of video-like camera to display an image on a computer. A laser line notch filter (NF) blocked out the laser-line scattered light from the sample and a 665 nm long-pass filter (LP) cut off the short-wavelength emission. Both filters were inserted at the front of the lens for imaging the NIR emission of the sample.

The experimental diagram of the steady-state spectroscopy setup is shown in Figure 2. The measurements were performed using a quarter meter spectrograph (ARC SpectroPro 275, Acton, MA) and a cooled CCD camera (Princeton Instrument model TE/CCD-512SF, Trenton, NJ). The laser beam was transmitted through a narrow band filter (NB) and focused by a 20-cm focal length lens (L_1) on the sample. The emitted light from the tissue sample was collected in the back-scattering geometry by an 85-mm focal length camera lens (L_2). After passing through a laser-line notch filter (NF), it was coupled into the 0.1-mm slit of a spectrograph, spectrally analyzed and recorded by the CCD camera.

The muscle samples from the chicken breast muscles were purchased from a local market and considered as

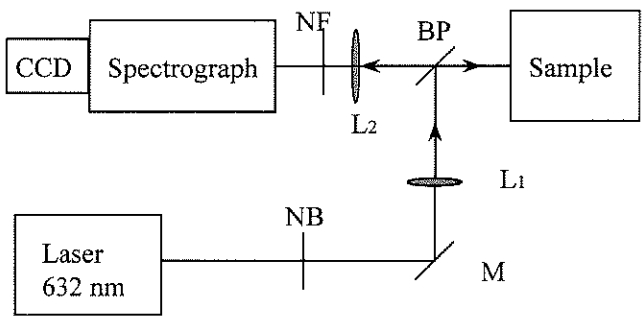

Fig. 2. Schematic diagrams of the steady-state spectroscopy experimental setup measurements. BP: beam splitter; NB: narrow band filter (laser line), L_1: excitation lens; L_2: signal collection lens; NF: notch filter (laser line).

homogeneous (on a macroscopic level) biological test media. After the fat and tendon tissues were removed, the samples were cut as a cylinder 4 mm in diameter and 1 mm in height, and were mounted in a glass slide for heating and spectral analysis.

Heating took place for 5 min in an oven (Furnace Type 48000, Barnstand/Thermolyne, Dubugue, IW) controlled by a temperature controller (Thermolyne), where temperature stability was $\pm 1°C$. The temperature was set at every 5°C step from 40°C until that of tissue burn-off. Since the thermal diffusion time for a 1-mm sample is approximately 1 sec [16], the 5-min heating time ensured that the temperature at the center of a 1-mm thick tissue sample approximated the surface temperature. The number of samples used in this study was 336. At each temperature level, six target sites were measured. After cooling down to room temperature (approximately 5 min after heating), the samples were set for the spectral emission intensity measurement. The measurement process was finished within 30 min after heating. The temperature of the optical measuring environment was 25°C (air-conditioned room temperature) and the humidity was 40–50%.

In another group, with one non-heat treated sample as well as samples heated at 50, 90, 130, 170, 210, and 250°C temperatures for 5 min were respectively measured with the steady-state emission spectroscopy setup (Fig. 2) for NIR emission spectral wing profiles.

In the third group, after the samples were heated at temperatures 50, 90, 130, 170, 210, and 250°C respectively, for 5 min, the emission intensity measurements were repeated every hour until the eighth hour and 24th, 48th, and 72nd hour. This group was used to detect the changes in the extent of emission intensity with time. Between each measurement, the sample was kept in the same room temperature (25°C) and the same room humidity (40–50%).

The spectral data were calibrated and analyzed with the aid of the V for Windows software (Digital Optics Ltd., Auckland, New Zealand). For simplicity and due to the fact that the intensity was virtually homogeneous, the emission intensity was measured by the maximum square drawn inside the circular sample surface. Data are expressed as the mean $\pm$ standard deviation (SD) throughout the text and figures.

For changes in the extent of emission intensity in each group, one-way ANOVA was performed. A p-value of < 0.05 was assumed to represent a significant difference.

RESULTS

Visual analysis of muscle samples revealed a steady progress of dehydration, coagulation, vaporization, carbonization, and tissue burn-off. When the temperature rose from 40 to 155°C, the color of the tissue became bleaching, turbid, and dry. While the temperature was from 160 to 210°C, the tissue changed in the color from yellowish to brown. When the temperature continued to rise, tissue color darkened and carbonization occurred. The tissue burn-off was at the temperature of 320°C.

The NIR emission spectral wing profiles (from 650 to 900 nm) from the samples with different temperature treatments are shown in Figure 3. The emission spectral profiles were similar in the tissue samples treated with different temperatures, except for a weak peak (~3,000 cm^{-1}) found around 770 nm at temperatures below 130°C and a small shoulder peak appeared around 720 nm at a temperature of 250°C. The 770-nm peak may be attributed to the Raman mode of water. The half width (HW) of the spectra profile has slight differencec with different temperature treatments. The HW became wider, when temperature was higher than 170°C. Stronger emission intensity at higher temperature treatment also was observed over a temperature range from reference (non-heat) to 250°C. The intensities of the spectral profile have about 3 order differences in this temperature range.

After normalizing emission intensity to the non-treated sample level, the curve describing the relative emission intensity of the heat-treated samples vs. temperature is plotted in Figure 4.

The relationship between relative emission intensity changes in heated tissue and treatment temperature is plotted in the left part of Figure 4. A linear relationship between the emission intensity from tissue samples and treatment temperature was observed on the four different temperature ranges: from 40 to 155°C, from 160 to 205°C, from 210 to 250°C, and from 255 to 290°C. The data were fitted by a linear equation for these separated regions:

$$I_N(T) = Io + b(T - To)$$

where T is the temperature of the treated tissue, $I_N(T)$ is the normalized emission intensity, which is defined as $I_E(T)/I_E$ (room temperature = 25°C), $I_E(T)$ is defined as the measured emission intensity of the sample at temperature T; Io is the normalized emission intensity of the sample at the initial onset temperature To; and b is the slope of the temperature-dependent emission intensity with the unit of per 1°C.

The relationship between emission intensity changes and time after heat application is plotted in Figure 5. For the samples with no-heat-treated and heat-treated at temperatures of 50°C and 90°C, the emission intensity increases during the first 8 hours, and then level off to a plateau. In the groups of the sample treated at temperatures of 130, 170, 210, and 250°C, the fluctuation of emission intensity decreased slightly during the first hour, especially in the group of samples at temperatures of 170, 210, and 250°C, then remained approximately at the same level during the experimental period.

DISCUSSION

From the data displayed in Figure 4, a functional relationship appears to exist between the intensity of the NIR emission and the extent of thermal action. The results show that emission intensity increases in response to the application of heat in the temperature range from 40 to 250°C, and sharp decrease in intensity when the tissue undergoes burn-off. The relative emission intensity of the heated tissue samples is linearly proportional to treatment temperature within the three temperature ranges: from 40 to 155°C, from 160 to 205°C, from 210 to 250°C, and from 255 to 290°C. The value of the emission intensity is stable for at least 72 hours after heat treatment.

$$Io_1 = 0.7419 \quad b_1 = 0.04252 \quad To_1 = 40°C \quad \text{for } 40°C < T < 155°C$$
$$Io_2 = 6.418 \quad b_2 = 2.960 \quad To_2 = 160°C \quad \text{for } 160°C < T < 205°C$$
$$Io_3 = 113.76 \quad b_3 = 15.537 \quad To_3 = 210°C \quad \text{for } 210°C < T < 250°C$$
$$Io_4 = 659.183 \quad b_4 = -18.375 \quad To_4 = 255°C \quad \text{for } 255°C < T < 290°C$$

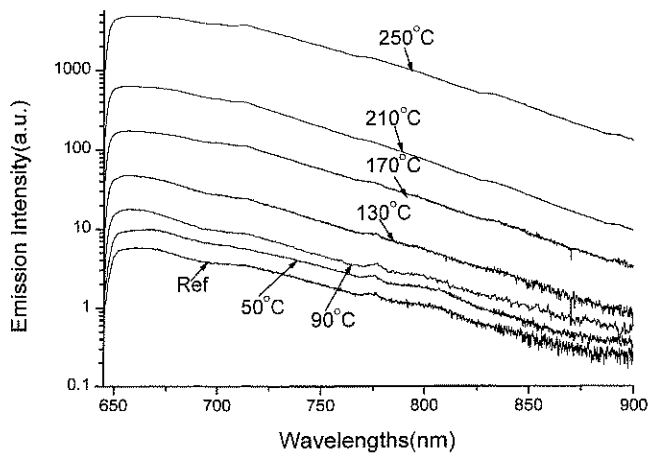

Fig. 3. NIR spectral profiles (650–900 nm) of the NIR emission from tissue samples treated with different temperatures: Ref. (no-heat), 50, 90, 130, 170, 210, and 250°C.

The increase in the emission intensity from the tissue after heat treatment is different in different temperature ranges. Some changes in protein structure may be correlated to emission intensity increase, such as that of collagen by heating [17]. It is known that when the temperature rises to 60°C, collagen denatures. Its helical structure becomes unfolded [13]. Another possible reason for the increase in emission efficiency is the change in the tertiary and/or secondary protein structures under thermal treatment due to hydrogen bond breakage and cross-link changes between the proteins [18]. The energy transfer channels in the protein are distorted by heat, which can induce a quantum efficiency of the fluorophores in the tissue. At the same time, there may be some other fluophores, which are inside the protein structure, to be exposed. The first protein structures begin to be altered or destroyed at these temperature levels. Most melting points

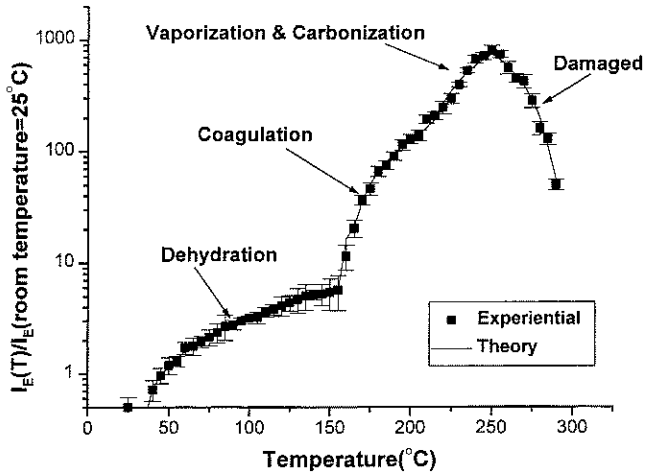

Fig. 4. Relative $[I_E(T)/I_E$ (room temperature = 25°C)] NIR emission from thermally treated tissue samples vs. treatment temperature. The data are plotted with a linear fitting approach. A linear relationship between emission intensity from tissue samples and treatment temperature is observed in the four different temperature ranges: from 40 to 155°C (dehydration), from 160 to 205°C (coagulation), from 210 to 250°C (vaporization and Carbonization), and from 255 to 290°C (damaged).

of amino acids are between 170 and 225°C [19]. The spectral profile modification indicates that there may be new fluophores being formed. With additional fluophores being formed with temperature increase, this may cause emission intensity to increase in the two different temperature ranges with different rates of intensity increase (from 165 to 220°C, and from 225 to 250°C). During these periods, tissue coagulation, vaporization, and carbonization occur. These changes in protein structure caused by heat are not reversible even as the tissue temperature returns to room temperature. The NIR emission intensity is comparable to the intensity of Raman scattering and this may indicate that this emission arises from non-dipole moment allowing electronic transitions [14]. Heating may alter the protein structures to cause less coupling and a reduction in non-radiative process. At treatment temperature rises above 250°C, these fluophores begin to be destroyed. Emission intensity decreases quickly until tissue is completely burned off.

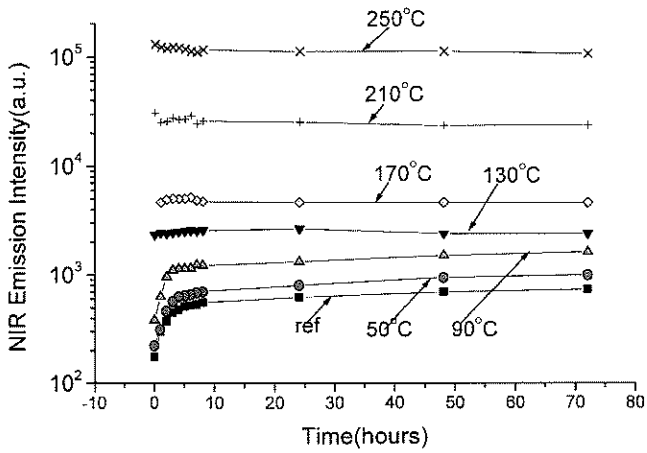

Fig. 5. Relative intensity of NIR emission changes from tissue samples heated to different temperatures and measured at times varying from every one hour until the eighth hour and 24th, 48th, 72nd hours after heat treatment.

Water in the tissue also can play an important role in influencing the tissue emission intensity in the first temperature range (temperature less than 170°C). We note that a non-heat-treated sample increases its emission intensity. The tissue loses its water in the air with time (see Fig. 5, the curve of non-heat-treated samples). The emission intensity of the tissue group at 50 and 90°C also increases due to continuous water loss in the air with time. The emission intensity of the samples treated at temperature higher than 170°C (see Fig. 5) decreases in the first hour. These treated tissues can "draw" water from the air after heat treatment.

The observed emission intensity changes in the tissue heat treatment below 160°C are attributed mainly to water loss. The first step of tissue ablation by heating is tissue dehydration. A high temperature would need to evaporate the substantial water in the tissue, if the heat time is short. LeCarpentier et al. [20] also noted that tissue dehydration without ablation occurs on tissue irradiated with a CW argon laser, when temperature rises from 130 to 140°C. Actually, during the tissue dehydration period, some protein structures can change. It was reported that water is intimately involved in the collagen structure [21]. Electron microscopy of the replicas of wet collagen shows relatively smooth cylindrical fibers in contrast to the corrugated appearance of dry collagen [22].

Our results show that the extent of thermal damage to tissue can be monitored non-invasively using NIR emission intensity measurement. Measurements of emission intensity on heated tissue could not only detect the extent of tissue damage after thermal injury, but also as a non-contact method to monitor temperature associated changes.

ACKNOWLEDGMENTS

This work is supported by the DOE Center of Excellence Program.

REFERENCES

1. Jain KK, Gorish W. Repair of small blood vessels with the neodymium YAG laser: a preliminary report. Surgery 1979;85:684–688.
2. Bass LS. Laser tissue welding: a comprehensive review of current and future clinical applications Lasers Surg Med 1995;17:315–349.
3. Maitinot VJ, Mordon SR, Mitchell VA, Pellerin PN, Brunetaud JM. Determination of efficient parameters for argon laser-assisted anastomoses in rats: macroscopic, thermal, and histological evaluation. Lasers Surg Med 1994;15:168–175.
4. Barbeau GR, Abela GS, Seeger JM, Friedl SE, Tomaru T, Giacomino PP. Temperature monitoring during peripheral thermo-optical laser recanalization in humans. Clin Cardiol 1990;13:690–697.

5. Bown SG. Phototherapy of tumors. World J Surg 1983;7:700–709.
6. Prudhomme M, Tang J, Rouy S, Delacretaz G, Salathe RP, Godlewski G. Interstitial diode laser hyperthermia in the treatment of subcutaneous tumor. Lasers Surg Med 1996;19: 445–450.
7. Robertson GS, Thomas M, Jamieson J, Veitch PS, Dennison AR. Palliation of oesophageal carcinoma using the argon beam coagulator. Br J Surg 1996;83:1769–1771.
8. Caspani B, Cecconi PR, Bottelli R, Della Vigna P, Ideo G, Gozzi G. The interstitial photocoagulation with laser light of liver tumors. Radiol Med (Torino) 1997;94:346–354.
9. Schober R, Bettage M, Sabel M, Ulrich F, Hessel S. Fine structure of zonal change in experimental Nd:YGY laser-induced interstitial hyperthermia. Lasers Surg Med 1993;13: 234–241.
10. Haines DE, Watson DD. Tissue heating during radio-frequency catheter ablation: a thermodynamic model and observations in isolated perfused and super-perfused canine right ventricular free wall. PACE 1989;12:962–976.
11. Haines DE, Watson DD, Verow AF. Electrode radius predicts lesion radius during radiofrequency energy heating. Circ Res 1990;67:124–129.
12. Dinerman, JL, Berger RD, Calkins H. Temperature monitoring during radiofrequency ablation. J Cardiovasc Electrophysiol 1996:7:163–173.
13. Thomsen S, Pearce JA, Cheong W. Changes in birefringence as markers of thermal damage in tissues. IEEE Trans Biomed Engin 1989;36:1174–1179.
14. Zhang G, Demos SG, Alfano RR. Far-red and NIR emission from tissues. SPIE Proceeding of Optical Biopsy II 1998;3250: 72–77.
15. Zhang G, Tang J, Ho PP, Alfano RR. Probing thermal damage and monitoring temperature of tissues using near-infrared emission intensity measurements. Laser in the Life Science 2000;9:95–109.
16. ven Gemert MJC, Welch AJ. Time constants in thermal laser medicine. Lasers Surg Med 1989;9:405–421.
17. Post MJ, de Graaf-Bos AN, Posthuma G, de Groot PG, Sixma JJ, Borst C. Interventional thermal injury of the arterial wall: unfolding of von Willebrand factor and its increased binding to collagen after 55°C heating. Thromb Haemost 1996;75:515–519.
18. Bailey AJ, Sims TJ, Avery NC, Miles CA. Chemistry of collagen cross-links: glucose-mediated covalent cross-linking of type-IV collagen in lens capsules. Biochem J 1993;296: 489–496.
19. Sober HA, Harte RA, Sober EK. Handbook of biochemistry. 2nd ed., The Chemical Rubber Co., Ohio, D-12.
20. LeCarpentier GL, Motamedi M, McMath LP, Rastegar S, Welch AJ. Continuous wave laser ablation of tissue: analysis of thermal and mechanical events. IEEE Trans on Biomed Eng 1993;40:188–220.
21. Luescher M. Effect of hydration upon the thermal stability of tropocollagen and its dependence on the presence of neutral salts. Biopolymers 1974;13:2489–2503.
22. Traub W, Piez K. The chemistry and structure of collagen. Adv Protein Chem 1971;25:320–325.

5. Bown SG. Phototherapy of tumors. World J Surg 1983;7:700–709.
6. Prudhomme M, Tang J, Rouy S, Delacretaz G, Salathe RP, Godlewski G. Interstitial diode laser hyperthermia in the treatment of subcutaneous tumor. Lasers Surg Med 1996;19: 445–450.
7. Robertson GS, Thomas M, Jamieson J, Veitch PS, Dennison AR. Palliation of oesophageal carcinoma using the argon beam coagulator. Br J Surg 1996;83:1769–1771.
8. Caspani B, Cecconi PR, Bottelli R, Della Vigna P, Ideo G, Gozzi G. The interstitial photocoagulation with laser light of liver tumors. Radiol Med (Torino) 1997;94:346–354.
9. Schober R, Bettage M, Sabel M, Ulrich F, Hessel S. Fine structure of zonal change in experimental Nd:YGY laser-induced interstitial hyperthermia. Lasers Surg Med 1993;13: 234–241.
10. Haines DE, Watson DD. Tissue heating during radio-frequency catheter ablation: a thermodynamic model and observations in isolated perfused and super-perfused canine right ventricular free wall. PACE 1989;12:962–976.
11. Haines DE, Watson DD, Verow AF. Electrode radius predicts lesion radius during radiofrequency energy heating. Circ Res 1990;67:124–129.
12. Dinerman, JL, Berger RD, Calkins H. Temperature monitoring during radiofrequency ablation. J Cardiovasc Electrophysiol 1996:7:163–173.
13. Thomsen S, Pearce JA, Cheong W. Changes in birefringence as markers of thermal damage in tissues. IEEE Trans Biomed Engin 1989;36:1174–1179.
14. Zhang G, Demos SG, Alfano RR. Far-red and NIR emission from tissues. SPIE Proceeding of Optical Biopsy II 1998;3250: 72–77.
15. Zhang G, Tang J, Ho PP, Alfano RR. Probing thermal damage and monitoring temperature of tissues using near-infrared emission intensity measurements. Laser in the Life Science 2000;9:95–109.
16. ven Gemert MJC, Welch AJ. Time constants in thermal laser medicine. Lasers Surg Med 1989;9:405–421.
17. Post MJ, de Graaf-Bos AN, Posthuma G, de Groot PG, Sixma JJ, Borst C. Interventional thermal injury of the arterial wall: unfolding of von Willebrand factor and its increased binding to collagen after 55°C heating. Thromb Haemost 1996;75:515–519.
18. Bailey AJ, Sims TJ, Avery NC, Miles CA. Chemistry of collagen cross-links: glucose-mediated covalent cross-linking of type-IV collagen in lens capsules. Biochem J 1993;296: 489–496.
19. Sober HA, Harte RA, Sober EK. Handbook of biochemistry. 2nd ed., The Chemical Rubber Co., Ohio, D-12.
20. LeCarpentier GL, Motamedi M, McMath LP, Rastegar S, Welch AJ. Continuous wave laser ablation of tissue: analysis of thermal and mechanical events. IEEE Trans on Biomed Eng 1993;40:188–220.
21. Luescher M. Effect of hydration upon the thermal stability of tropocollagen and its dependence on the presence of neutral salts. Biopolymers 1974;13:2489–2503.
22. Traub W, Piez K. The chemistry and structure of collagen. Adv Protein Chem 1971;25:320–325.